On the computation of directional scale-discretized wavelet transforms on the sphere

Jason D. McEwen[a,b], Pierre Vandergheynst[c] and Yves Wiaux[c,d,e]

[a] Department of Physics and Astronomy, University College London (UCL),
London WC1E 6BT, UK
[b] Mullard Space Science Laboratory (MSSL), University College London (UCL),
Surrey RH5 6NT, UK
[c] Institute of Electrical Engineering, Ecole Polytechnique Fédérale de Lausanne (EPFL),
Lausanne 1015, Switzerland;
[d] Department of Medical Radiology, University Hospital Center (CHUV) and University of
Lausanne (UNIL), CH-1011 Lausanne, Switzerland;
[e] Department of Radiology and Medical Informatics, University of Geneva (UniGE),
Geneva 1211, Switzerland

ABSTRACT

We review scale-discretized wavelets on the sphere, which are directional and allow one to probe oriented structure in data defined on the sphere. Furthermore, scale-discretized wavelets allow in practice the exact synthesis of a signal from its wavelet coefficients. We present exact and efficient algorithms to compute the scale-discretized wavelet transform of band-limited signals on the sphere. These algorithms are implemented in the publicly available S2DW code. We release a new version of S2DW that is parallelized and contains additional code optimizations. Note that scale-discretized wavelets can be viewed as a directional generalization of needlets. Finally, we outline future improvements to the algorithms presented, which can be achieved by exploiting a new sampling theorem on the sphere developed recently by some of the authors.

Keywords: Sphere, sampling theorem, wavelet transform.

1. INTRODUCTION

Wavelets on the sphere have found widespread application in fields such as cosmology (*e.g.* Ref. 1) and geophysics (*e.g.* Ref. 2), where data are observed on a spherical domain. The ability of wavelets to probe spatially localized, scale-dependent features in signals has become an instrumental tool to relate data to physical theories, as many physical processes are spatially localised but manifest on particular physical scales. Since such data-sets are of considerable size, often containing tens of millions of pixels, efficient algorithms are also of central importance.

Many wavelet transforms on the sphere have been developed.[3–15] Of particular note are so-called needlets, which have been applied extensively to the analysis of observations of the cosmic microwave background (CMB). Needlets have found broad application since they exhibit many useful properties and the needlet transform can be computed relatively straightforwardly. However, needlets are axisymmetric wavelets and thus cannot be used to probe directional or oriented structure in data on the sphere.

In this article we review the scale-discretized wavelets on the sphere developed by Wiaux *et al.*,[16] which were developed independently of needlets, about the same time, and which share many of the useful properties of needlets. However, scale-discretized wavelets are also directional, allowing one to probe oriented structure in data. Directional wavelets are very useful for the analysis of signals on the sphere with oriented structure; for example, the CMB fluctuations induced by cosmic strings,[17, 18] a well-motivated but as yet unobserved phenomenon.

Further author information:
JDM: E-mail: jason.mcewen@ucl.ac.uk, URL: http://www.jasonmcewen.org/

In addition to reviewing scale-discretized wavelets on the sphere, we present exact and efficient algorithms to compute the corresponding wavelet analysis and synthesis, *i.e.* the forward and inverse wavelet transform respectively. These algorithms are implemented in the publicly available `S2DW`* code. Although the `S2DW` package has been available publicly for some time, these algorithms have not yet been described in the literature. Furthermore, we release a new version (1.1) of `S2DW` that is parallelized and contains additional code optimizations.

The remainder of this article is organized as follows. In Sec. 2 we review the scale-discretized wavelet transform on the sphere. In Sec. 3 we present our algorithms to compute the wavelet transform exactly and efficiently. Numerical experiments are also performed to evaluate the speed and accuracy of the algorithms. Concluding remarks are made in Sec. 4, where we also outline future optimizations of the algorithms by exploiting recent developments[19] made by some of the authors pertaining to sampling theorems on the sphere.

2. DIRECTIONAL SCALE-DISCRETIZED WAVELETS

The directional scale-discretized wavelet transform supports the analysis of oriented spatially localised, scale-dependent features in signals on the sphere. In this section we review the scale-discretized wavelet framework on the sphere developed by Wiaux *et al.*.[16] Firstly, we review the wavelet transform itself, before secondly reviewing the construction of admissible scale-discretized wavelets.

2.1 Wavelet transform

The scale-discretized wavelet transform of a function $f \in \mathrm{L}^2(\mathbb{S}^2)$ on the sphere $\mathbb{S}^2$ is defined by the directional convolution of f with the wavelet $\Psi^j \in \mathrm{L}^2(\mathbb{S}^2)$. The wavelet coefficients $W^{\Psi^j} \in \mathrm{L}^2(\mathrm{SO}(3))$ thus read

$$W^{\Psi^j}(\rho) \equiv (f \star \Psi^j)(\rho) = \langle f, \mathcal{R}_\rho \Psi^j \rangle = \int_{\mathbb{S}^2} \mathrm{d}\Omega(\omega) f(\omega)(\mathcal{R}_\rho \Psi^j)^*(\omega) \,, \tag{1}$$

where $\omega = (\theta, \varphi) \in \mathbb{S}^2$ denotes spherical coordinates with colatitude $\theta \in [0, \pi]$ and longitude $\varphi \in [0, 2\pi)$, $\mathrm{d}\Omega(\omega) = \sin\theta \, \mathrm{d}\theta \, \mathrm{d}\varphi$ is the usual rotation invariant measure on the sphere, and $\cdot^*$ denotes complex conjugation. The rotation operator is defined by

$$(\mathcal{R}_\rho \Psi^j) \equiv \Psi^j(\mathbf{R}_\rho^{-1} \cdot \omega) \,, \tag{2}$$

where $\mathbf{R}_\rho$ is the three-dimensional rotation matrix corresponding to $\mathcal{R}_\rho$. Rotations are specified by elements of the rotation group SO(3), parameterized by the Euler angles $\rho = (\alpha, \beta, \gamma) \in \mathrm{SO}(3)$, with $\alpha \in [0, 2\pi)$, $\beta \in [0, \pi]$ and $\gamma \in [0, 2\pi)$. We adopt the *zyz* Euler convention corresponding to the rotation of a physical body in a *fixed* coordinate system about the z, y and z axes by γ, β and α, respectively. The wavelet transform Eqn. (1) thus probes directional structure in the signal of interest f, where γ corresponds to the orientation about each point on the sphere $(\theta, \varphi) = (\beta, \alpha)$.

The wavelet scale $j \in \mathbb{N}_0$ encodes the localization extent of Ψ^j, which is closely related to the wavelet construction and is discussed in Sec. 2.2. For now it is sufficient to note that the wavelet scales j are discrete (hence the name scale-discretized wavelets), which affords the exact synthesis of a function from its wavelet (and scaling) coefficients.

The wavelet coefficients encode only the high-frequency, detail information contained in the signal f; scaling coefficients must be introduced to represent the low-frequency, approximation information of the signal. The scaling coefficients $W^\Phi \in \mathrm{L}^2(\mathbb{S}^2)$ are given by the convolution of f with the axisymmetric scaling function $\Phi \in \mathrm{L}^2(\mathbb{S}^2)$ and read

$$W^\Phi(\omega) \equiv (f \star \Phi)(\omega) = \langle f, \mathcal{R}_\omega \Phi \rangle = \int_{\mathbb{S}^2} \mathrm{d}\Omega(\omega') f(\omega')(\mathcal{R}_\omega \Phi)^*(\omega') \,, \tag{3}$$

where $\mathcal{R}_\omega = \mathcal{R}_{(\varphi, \theta, 0)}$. Note that the scaling coefficients live on the sphere, and not the rotation group SO(3), since we do not probe the directional structure of the low-frequency, approximation information of f. An extension to a directional scaling function could be made trivially, however it is not of significant practical use. Typically, a

---

signal of interest is decomposed into its scaling and wavelet coefficients and the wavelet coefficients are analyzed or manipulated, while the scaling coefficients remain untouched.

Provided an admissibility condition holds, the signal f can be synthesised perfectly from its wavelet and scaling coefficients by

$$f(\omega) = 2\pi \int_{\mathbb{S}^2} \mathrm{d}\Omega(\omega')W^\Phi(\omega')(\mathcal{R}_{\omega'}L^\mathrm{d}\Phi)(\omega) + \sum_{j=0}^J \int_{\mathrm{SO}(3)} \mathrm{d}\varrho(\rho)W^{\Psi^j}(\rho)(\mathcal{R}_\rho L^\mathrm{d}\Psi^j)(\omega) ,\qquad(4)$$

where $\mathrm{d}\varrho(\rho) = \sin\beta\,\mathrm{d}\alpha\,\mathrm{d}\beta\,\mathrm{d}\gamma$ is the usual invariant measure on $\mathrm{SO}(3)$ and J is the maximum analysis depth considered, $i.e.$ $0 \leq j \leq J$ (discussed in more detail in Sec. 2.2). The operator L^d is defined by its action on the harmonic coefficients of functions $h \in \mathrm{L}^2(\mathbb{S}^2)$:

$$(L^\mathrm{d}h)_{\ell m} \equiv \frac{2\ell + 1}{8\pi^2}h_{\ell m} .\qquad(5)$$

where $h_{\ell m} = \langle h, Y_{\ell m}\rangle$ are the spherical harmonic coefficients of h and $Y_{\ell m} \in \mathrm{L}^2(\mathbb{S}^2)$ are the spherical harmonics[20] with $\ell \in \mathbb{N}_0$ and $m \in \mathbb{Z}$, such that $|m| \leq \ell$.

The admissibility condition under which a function f can be synthesised perfectly from its wavelet and scaling coefficients is given by the following resolution of the identity:

$$|\Phi_{\ell 0}|^2 + \sum_{j=0}^J \sum_{m=-\ell}^\ell |\Psi_{\ell m}^j|^2 = 1 , \quad \forall\ell ,\qquad(6)$$

where $\Phi_{\ell 0}\delta_{m0} = \langle \Phi, Y_{\ell m}\rangle$ and $\Psi_{\ell m}^j = \langle \Psi, Y_{\ell m}\rangle$ are the spherical harmonic coefficients of Φ and Ψ^j, respectively. Typically, we consider band-limited functions, $i.e.$ functions such that $f_{\ell m} = 0$, $\forall\ell \geq L$, where $f_{\ell m} = \langle f, Y_{\ell m}\rangle$, for which case wavelet analysis and synthesis can be computed exactly in practice (see Sec. 3).

2.2 Wavelet construction

The scale-discretized wavelets are constructed in such a way to ensure the admissibility criterion Eqn. (6) is satisfied. Furthermore, the wavelets are defined in harmonic space in the factorized form:

$$\Psi_{\ell m}^j \equiv \kappa^j(\ell)s_{\ell m} ,\qquad(7)$$

in order to essentially control their angular and directional localization separately, through the kernel κ^j and directionality component, with harmonic coefficients $s_{\ell m}$, respectively; we discuss each in turn.

Without loss of generality, the directionality component $s \in \mathrm{L}^2(\mathbb{S}^2)$, with harmonic coefficients $s_{\ell m} = \langle s, Y_{\ell m}\rangle$, is defined to impose

$$\sum_{|m| \leq \ell} |s_{\ell m}|^2 = 1 ,\qquad(8)$$

for all values of ℓ for which $s_{\ell m}$ are non-zero for at least one value of m. The angular localisation properties of the wavelet Ψ^j are then controlled largely by the kernel and to a lesser extent by the directional component, while the directional component controls precisely the directional properties of the wavelet ($i.e.$ the behaviour of the wavelet with respect to the azimuthal variable φ, when centered on the North pole). Furthermore, we impose the zero-mean condition $s_{00} = 0$ and an azimuthal band-limit N on the directional component such that $s_{\ell m} = 0$, $\forall\ell, m$ with $|m| \geq N$.

As soon as one imposes an azimuthal band-limit, one recovers steerable wavelets,[13, 16, 21] where the wavelet rotated about itself ($i.e.$ rotated about the z axis when centered on the North pole) can be expressed as a finite weighted linear combination of wavelets specified at base orientations. This property is expressed equivalently on the directional component s by

$$s_\gamma(\omega) = \sum_{g=0}^{M-1} z(\gamma - \gamma_g)s_{\gamma_g}(\omega) ,\qquad(9)$$

where $s_\gamma \equiv \mathcal{R}_{(0,0,\gamma)}s$. The rotation angles γ_g are equispaced and are defined explicitly in Sec. 3.1. We consider wavelets with even or odd azimuthal symmetry (*i.e.* even or odd symmetry when rotated about itself by π, when centered on the North pole), in which case $M = N$. The interpolating function $z(\gamma)$ is independent of s and is defined by its Fourier coefficients z_n which take particularly simple forms for wavelets with even/odd azimuthal symmetry (see Ref. 16 for further detail). Due to the linearity of the wavelet transform, the steerability property is transferred to the wavelet coefficients themselves, yielding

$$W^{\Psi^j}(\alpha, \beta, \gamma) = \sum_{g=0}^{M-1} z(\gamma - \gamma_g) W^{\Psi^j}(\alpha, \beta, \gamma_g) . \tag{10}$$

Steerability is thus a very useful property for practical applications; for examples of steerable wavelet analyses on the sphere see Refs. 22, 23.

Following Ref. 16 we define the directionality coefficients to satisfy the criteria just discussed but also to ensure a convenient form for the directional auto-correlation function of the wavelet, yielding

$$s_{\ell m} = \eta_N \beta_{(N,m)} \sqrt{\frac{1}{2^{\gamma_{(N,\ell)}}} \binom{\gamma_{(N,\ell)}}{\frac{\gamma_{(N,\ell)}-m}{2}}} , \tag{11}$$

with $\eta_N = 1$ for even values of $N - 1$, $\eta_N = i = \sqrt{-1}$ for odd values of $N - 1$, $\beta_{(N,m)} = (1 - (-1)^{N+m})/2$, and $\gamma_{(N,\ell)} = \min\{N - 1, \ell - (1 + (-1)^{N+\ell})/2\}$. With this definition one also recovers a wavelet with odd (even) azimuthal symmetry for N even (odd).

The kernel $\kappa^j(t)$ is a positive real function, with argument $t \in \mathbb{R}$, although $\kappa(t)$ is only evaluated for natural arguments $t = \ell$ in Eqn. (7). The kernel controls the angular localization of the wavelet and is constructed to be a smooth function with compact support, as follows. Consider the infinitely differentiable Schwartz function with compact support $t \in [\alpha^{-1}, 1]$, for dilation parameter $\alpha \in \mathbb{R}_*^+$, $\alpha > 1$:

$$s_\alpha(t) \equiv s\left(\frac{2\alpha}{\alpha - 1}(t - \alpha^{-1}) - 1\right), \quad \text{with} \quad s(t) \equiv \begin{cases} \exp(-(1 - t^2)^{-1}), & t \in [-1, 1] \\ 0, & t \notin [-1, 1] \end{cases} . \tag{12}$$

We then define the smoothly decreasing function k_α by

$$k_\alpha(t) \equiv \frac{\int_t^1 \frac{\mathrm{d}t'}{t'} s_\alpha^2(t')}{\int_{\alpha^{-1}}^1 \frac{\mathrm{d}t'}{t'} s_\alpha^2(t')}, \tag{13}$$

which is unity for $t < \alpha^{-1}$, zero for $t > 1$, and is smoothly decreasing from unity to zero for $t \in [\alpha^{-1}, 1]$. We define the wavelet kernel generating function by

$$\kappa_\alpha(t) \equiv \sqrt{k_\alpha(\alpha^{-1}t) - k_\alpha(t)} , \tag{14}$$

which has compact support $t \in [\alpha^{-1}, \alpha]$ and reaches a peak of unity at $t = 1$. The scale-discretized wavelet kernel for scale j is then defined by

$$\kappa^j(\ell) \equiv \kappa_\alpha(\alpha^j L^{-1} \ell) , \tag{15}$$

which has compact support on $\ell \in \left[\lfloor \alpha^{-(1+j)}L \rfloor, \lceil \alpha^{1-j}L \rceil\right]$, where $\lfloor \cdot \rfloor$ and $\lceil \cdot \rceil$ are the floor and ceiling functions respectively, and reaches a peak of unity at $\alpha^{-j}L$.[†] With this construction the kernel functions tile the harmonic line, as illustrated in Fig. 1.

The maximum possible wavelet scale $J_L(\alpha)$ is given by the lowest integer j for which the kernel peak occurs at or below $\ell = 1$, *i.e.* by the lowest integer value such that $\alpha^{-J_L(\alpha)}L \leq 1$, yielding $J_L(\alpha) = \lceil \log_\alpha(L) \rceil$. All

---

[†]We adopt the same definition as Ref. 16 for the wavelet scales j, with increasing j corresponding to larger angular scales, *i.e.* lower frequency content. Note that this differs to the definition adopted in Ref. 7 where increasing j corresponds to smaller angular scales but higher frequency content.
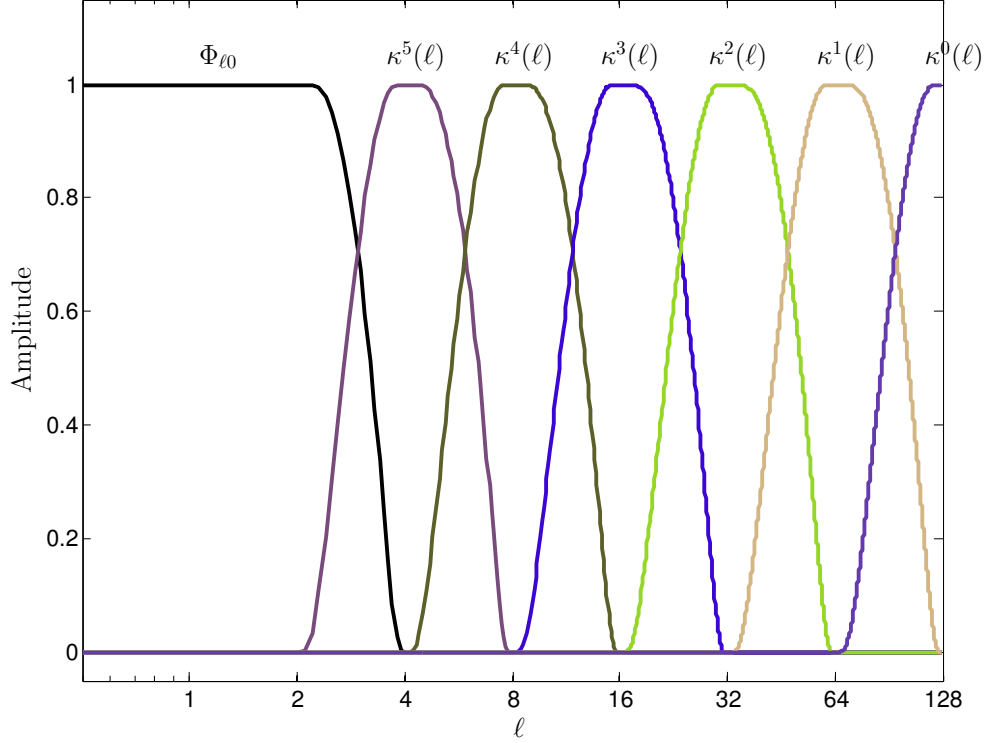
Figure 1. Scale-discretized wavelet tiling in harmonic space ($L = 128$, $N = 3$, $J = 5$, $\alpha = 2$).

wavelets for $j > J_L(\alpha)$ would be identically null as their kernel would have compact support in $\ell \in (0, 1)$. The maximum scale to be probed by the wavelets J can be chosen within the range $0 \leq J \leq J_L(\alpha)$. For $J = J_L(\alpha)$ the wavelets probe the entire frequency content of the signal of interest f except its mean, encoded in f_{00}.

To represent the signal content not probed by the wavelets the scaling function Φ is required, as discussed previously. Recall that the scaling function Φ is chosen to be axisymmetric; hence, we define the harmonic coefficients of the scaling function by

$$\Phi_{\ell 0} \equiv \sqrt{k_\alpha(\alpha^J L^{-1} \ell)}\,, \tag{16}$$

in order to ensure the scaling function probes the signal content not probed by the wavelets.

For the wavelets, scaling function and scale parameter ranges outlined above, the admissibility criterion Eqn. (6) is satisfied. Example directional scale-discretized wavelets are plotted in Fig. 2.

3. EXACT AND EFFICIENT COMPUTATION

We describe in this section the algorithms implemented in the S2DW[‡] package to support the exact and efficient computation of the scale-discretized wavelet transform on the sphere. We focus on the case of band-limited signals, which admit exact quadrature rules for certain discretizations of the sphere $\mathbb{S}^2$ and rotation group SO(3), leading to the exact computation of wavelet analysis and synthesis, *i.e.* forward and inverse transforms, respectively. Furthermore, we exploit the factoring of rotations approach to develop fast algorithms for both analysis and synthesis. Finally, we perform numerical experiments to illustrate the speed and accuracy of the algorithms developed.
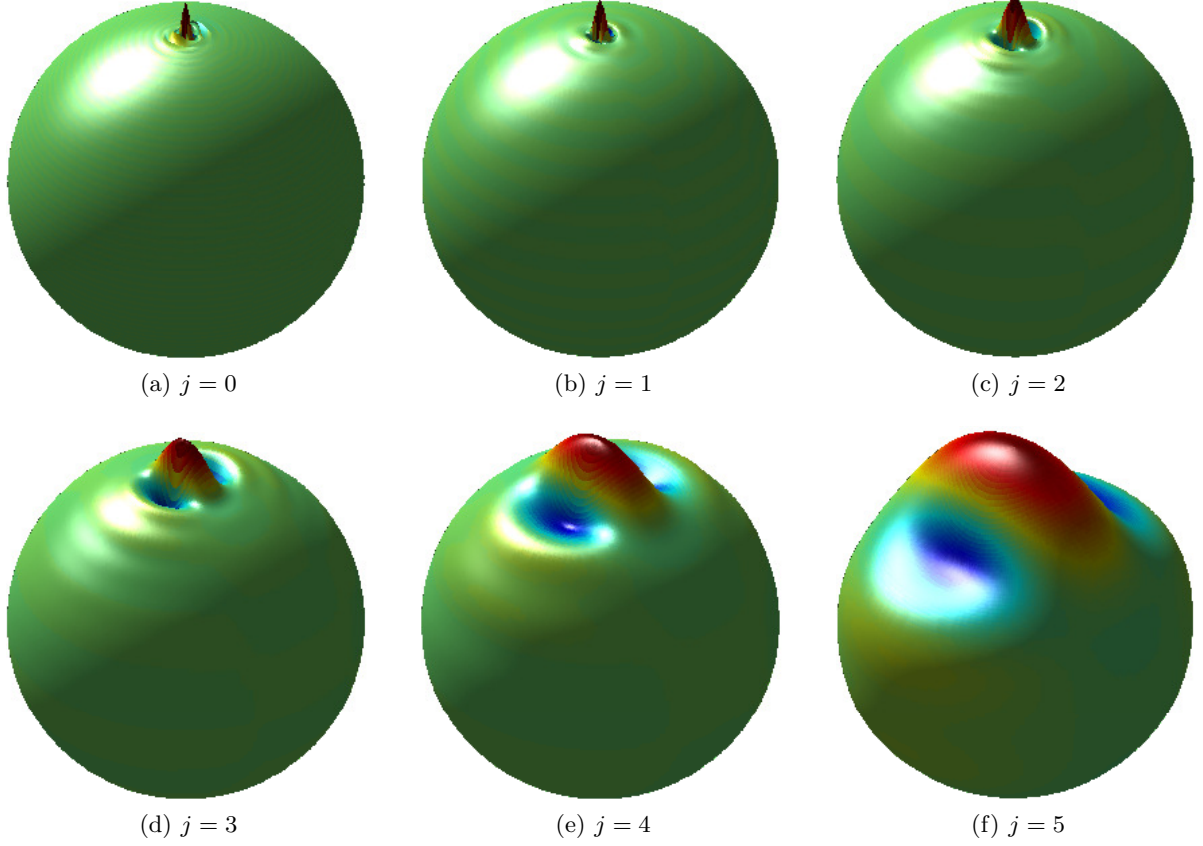

[‡] http://www.s2dw.org/

(a) $j = 0$ (b) $j = 1$ (c) $j = 2$

(d) $j = 3$ (e) $j = 4$ (f) $j = 5$

Figure 2. Parametric plots of scale-discretized wavelets on the sphere ($L = 128$, $N = 3$, $J = 5$, $\alpha = 2$).

3.1 Discretization and quadrature

The Driscoll and Healy sampling theorem[24, 25] is adopted in S2DW, with the corresponding cubature points: $\theta_t = \pi(2t + 1)/(4L)$, for $t = 0, \ldots, 2L - 1$, and $\varphi_p = 2\pi p/(2L - 1)$, for $p = 0, \ldots, 2L - 2$, giving $4L^2$ samples on the sphere. The Driscoll and Healy sampling theorem can be distilled into the following quadrature rule for the *exact* integration over colatitude θ of a function f band-limited at $2L$ or below:

$$\int_0^\pi \mathrm{d}\theta \sin\theta \, f(\theta, \cdot) = \sum_{t=0}^{2L-1} q(\theta_t) f(\theta_t, \cdot) \,, \tag{17}$$

where the quadrature weights are given by[24–26]

$$q(\theta_t) = \frac{2}{L} \sin\theta_t \sum_{k=0}^{L-1} \frac{\sin((2k + 1)\theta_t)}{2k + 1} \,. \tag{18}$$

We will also make use of exact quadrature for the following integration over longitude φ, for a function f band-limited at L:

$$\int_0^{2\pi} \mathrm{d}\varphi \exp(-im\varphi) f(\cdot, \varphi) = \frac{2\pi}{2L - 1} \sum_{p=0}^{2L-2} \exp(-im\varphi_p) f(\cdot, \varphi_p) \,, \tag{19}$$

which follows from the continuous and discrete orthogonality of the complex exponentials.

We have so far considered the discretization of functions defined on the sphere $\mathbb{S}^2$; however, the wavelet coefficients themselves are defined on the rotation group SO(3) (due to the directional nature of the wavelet

transform). The Euler angles $\rho = (\alpha, \beta, \gamma)$ that parameterize SO(3) can be discretized by making the association to the sphere $(\beta_b, \alpha_a) = (\theta_t, \varphi_p)$, where the indices a and b vary over the same range as p and t respectively, and by discretizing γ by $\gamma_g = \pi g/N$, for $g = 0, \ldots, N-1$. Note that the wavelets constructed in Sec. 2.2 are invariant under an azimuthal rotation by π (when centered on the North pole), hence it is only necessary to discretize γ in the range $[0, \pi)$.

Finally, we note that in order to recover exactness for the wavelet analysis and synthesis algorithms that follow, we assume that the spherical harmonic coefficients of the function of interest can be computed exactly by appealing to a sampling theorem on the sphere (*e.g.* the Driscoll & Healy sampling theorem[24, 25]). In this setting all algorithms are theoretically exact. If a sampling theorem is not available for the particular pixelization of the sphere on which samples are taken (*e.g.* if one adopts the `HEALPix` pixelization scheme[27]), harmonic coefficients can nevertheless be computed approximately and the algorithms presented below applied.

3.2 Wavelet analysis

The wavelet analysis given by Eqn. (1) may be expressed in harmonic space by

$$W^{\Psi^j}(\rho) = \sum_{\ell=0}^{\infty} \sum_{m=-\ell}^{\ell} \sum_{n=-\ell}^{\ell} f_{\ell m} \Psi_{\ell n}^{j*} D_{mn}^{\ell*}(\rho) \tag{20}$$

where the Wigner D-functions D_{mn}^{ℓ} are the matrix elements of the irreducible unitary representation of the rotation group SO(3). Consequently, the $D_{mn}^{\ell*}$ also form an orthogonal basis in $\mathrm{L}^2(\mathrm{SO}(3))$. Since we consider functions band-limited at L and directional wavelets with azimuthal band-limit N in what follows, the upper limits of the summation over ℓ in Eqn. (20) can be truncated to $L-1$ and the upper (lower) limit in the summation over n can be truncated to $N-1$ $(-N+1)$. Subsequently, we use the shorthand notation $\sum_{\ell mn}$ to represent this case. In general, for the sake of brevity and readability we do not specify the limits of summation in the following, since the limits can be inferred easily. Since the computation of wavelet coefficients is expressed in Eqn. (20) as a finite sum rather than an integral (thanks for the orthogonality of the spherical harmonics), the wavelet coefficients may be computed exactly.

Wavelet analysis can be seen as an inverse Wigner transform, where the Wigner coefficients corresponding to the wavelet coefficients are given by

$$\left(W^{\Psi^j}\right)_{mn}^{\ell} = \frac{8\pi^2}{2\ell+1} f_{\ell m} \Psi_{\ell n}^{j*}. \tag{21}$$

Note that we have adopted the following convention for the Wigner transform: a function $g \in \mathrm{L}^2(\mathrm{SO}(3))$ may be expanded in terms of the basis functions $D_{mn}^{\ell*}$ by

$$g(\rho) = \sum_{\ell} \frac{2\ell+1}{8\pi^2} \sum_{mn} g_{mn}^{\ell} D_{mn}^{\ell*}(\rho), \tag{22}$$

where the Wigner coefficients are given by

$$g_{mn}^{\ell} = \langle g, D_{mn}^{\ell*} \rangle = \int_{\mathrm{SO}(3)} \mathrm{d}\varrho(\rho) g(\rho) D_{mn}^{\ell}(\rho). \tag{23}$$

Wavelet analysis can be computed efficiently using the factoring of rotations approach[9, 28, 29] as first suggest and computed in Ref. 9. We note the D-function decomposition in terms of the real d-functions:[20]

$$D_{mn}^{\ell}(\alpha, \beta, \gamma) = \exp(-im\alpha) \, d_{mn}^{\ell}(\beta) \exp(-in\gamma), \tag{24}$$

and the Fourier expansion of the d_{mn}^{ℓ}:

$$d_{mn}^{\ell}(\beta) = \exp(-i(n-m)\pi/2) \sum_{m'} \Delta_{m'm}^{\ell} \Delta_{m'n}^{\ell} \exp(-im'\beta), \tag{25}$$

which follows by a factoring of rotations,[9,28,29] where $\Delta_{mn}^\ell = d_{mn}^\ell(\pi/2)$. Substituting these expressions into Eqn. (20) and interchanging the order summation, one finds:

$$W^{\Psi^j}(\rho) = \sum_{mm'n} U_{mm'n} \exp(i(m\alpha + m'\beta + n\gamma)),\qquad(26)$$

where

$$U_{mm'n} = \exp(i(n-m)\pi/2) \sum_\ell \Delta_{m'm}^\ell \Delta_{m'n}^\ell f_{\ell m} \Psi_{\ell n}^{j*}.\qquad(27)$$

The first step of the fast wavelet analysis algorithm is to compute $U_{mm'n}$ via Eqn. (27), which can be computed with asymptotic complexity $\mathcal{O}(NL^3)$. The next step is to compute wavelet coefficients from $U_{mm'n}$ via Eqn. (26). In Ref. 9 a three-dimensional fast Fourier transform (FFT) was applied to perform this computation efficiently. However, in that setting the discretization of the Euler angles (α, β, γ) was largely arbitrary since wavelet synthesis was not considered (indeed, not possible in practice due to the continuous nature of the wavelet transform considered). Here we must evaluate the wavelet coefficients at the sample positions for which we have exact quadrature rules, as outlined in Sec. 3.1. We thus consider each Euler angle in turn and perform a separation of variables to compute Eqn. (26) efficiently.

Firstly, consider the Euler angle γ:

$$U_{mm'}(\gamma) = \sum_n U_{mm'n} \exp(in\gamma).\qquad(28)$$

Since the domain of interest for γ is $[0, \pi)$ and the azimuthal band-limit N is often very low, *i.e.* $N \ll L$, this summation is computed explicitly, with complexity $\mathcal{O}(N^2 L^2)$.

Next, consider the Euler angle β:

$$U_m(\beta, \gamma) = \sum_{m'} U_{mm'}(\gamma) \exp(im'\beta).\qquad(29)$$

Since we discretize β at the sample positions supported by the Driscoll and Healy sampling theorem, as specified in Sec. 3.1, this summation is also computed explicitly, with complexity $\mathcal{O}(NL^3)$.

Finally, consider the Euler angle α:

$$W^{\Psi^j}(\rho) = \sum_m U_m(\beta, \gamma) \exp(im\alpha).\qquad(30)$$

Since we are free to choose the discretization of α we ensure our choice is compatible with an FFT, so that the complexity of this computation is reduced from $\mathcal{O}(NL^3)$ for a direct computation to $\mathcal{O}(NL^2 \log L)$ by application of an FFT.

To summarise, wavelet analysis given by Eqn. (1) can be computed exactly by its representation as a discrete sum in harmonic space. Furthermore, we have described a fast algorithm for the exact computation of wavelet coefficients by performing a factoring of rotations and separation of variables. This fast algorithm reduces the complexity of computing wavelet coefficients for a given scale j from $\mathcal{O}(L^5)$ to $\mathcal{O}(NL^3)$. Since $J + 1$ wavelet scales are considered, the overall complexity of computing all wavelet coefficients is $\mathcal{O}(JNL^3)$. However, since the wavelets themselves have compact support it is not necessary to perform all wavelet transforms at the full band-limit L. Furthermore, the lower support of the wavelets can also be exploited to increase computational efficiency. Following these optimizations the computation is dominated by the largest two scales. Hence, the overall complexity of computing all wavelet transforms for all scales is effectively $\mathcal{O}(NL^3)$.

We close this discussion of the computation of the wavelet transform by noting that scaling coefficients can also be computed exactly and efficiently. Since the scaling coefficients are given by an axisymmetric convolution via Eqn. (3), their harmonic coefficients are given by

$$W_{\ell m}^\Phi = \sqrt{\frac{4\pi}{2\ell + 1}} f_{\ell m} \Phi_{\ell 0}^*,\qquad(31)$$

which can be computed in $\mathcal{O}(L^2)$. The scaling coefficients can then be computed exactly in real space by appealing to a sampling theorem on the sphere.

3.3 Wavelet synthesis

We first consider the contribution to the wavelet synthesis expression of Eqn. (4) from the wavelet coefficients. Expressing this contribution in harmonic space one finds:

$$\sum_{j=0}^{J} \int_{SO(3)} \mathrm{d}\varrho(\rho) W^{\Psi^j}(\rho)(\mathcal{R}_\rho L^\mathrm{d} \Psi^j)(\omega) = \sum_{j=0}^{J} \sum_{\ell m n} \frac{2\ell+1}{8\pi^2} \left(W^{\Psi^j}\right)_{mn}^{\ell} \Psi_{\ell n}^j Y_{\ell m}(\omega) \,, \tag{32}$$

where

$$\left(W^{\Psi^j}\right)_{mn}^{\ell} = \langle W^{\Psi^j}, D_{mn}^{\ell*} \rangle = \int_{SO(3)} \mathrm{d}\varrho(\rho) W^{\Psi^j}(\rho) D_{mn}^{\ell}(\rho) \,. \tag{33}$$

Thus, the wavelet coefficient contribution to the function synthesis can be computed exactly by Eqn. (32), with complexity $\mathcal{O}(NL^2)$ for each j (we consider all j at the end of this subsection) to compute the contribution to the harmonic coefficients $f_{\ell m}$, provided the Wigner coefficients $\left(W^{\Psi^j}\right)_{mn}^{\ell}$ can be computed exactly. We therefore turn our attention to the exact and efficient computation of Eqn. (33).

Eqn. (33) can also be computed efficiently using the factoring of rotations approach and a separation of variables. Substituting the D-function decomposition Eqn. (24) and the Fourier expansion of d_{mn}^{ℓ} Eqn. (25), Eqn. (33) reads

$$\left(W^{\Psi^j}\right)_{mn}^{\ell} = \exp(-i(n-m)\pi/2) \sum_{m'} \Delta_{m'm}^{\ell} \Delta_{m'n}^{\ell} V_{mm'n} \,, \tag{34}$$

where

$$V_{mm'n} = \int_{SO(3)} \mathrm{d}\varrho(\rho) W^{\Psi^j}(\alpha,\beta,\gamma) \exp(-i(m\alpha + m'\beta + n\gamma)) \,. \tag{35}$$

Note that Eqn. (34) can be computed exactly with complexity $\mathcal{O}(NL^3)$. We next appeal to the quadrature rules described in Sec. 3.1 to evaluate Eqn. (35) exactly, considering each Euler angle in turn.

Firstly, consider the Euler angle α. Appealing to the quadrature rule Eqn. (19), Eqn. (35) may be written:

$$V_{mm'n} = \int_0^\pi \mathrm{d}\beta \sin\beta \int_0^{2\pi} \mathrm{d}\gamma \, V_m(\beta,\gamma) \exp(-i(m'\beta + n\gamma)) \,, \tag{36}$$

where

$$V_m(\beta,\gamma) = \frac{2\pi}{2L-1} \sum_a W^{\Psi^j}(\alpha_a, \beta, \gamma) \exp(-im\alpha_a) \,. \tag{37}$$

The Euler angle α is discretized according to the scheme specified in Sec. 3.1, where a denotes the index associated with α. Naively Eqn. (37) may be computed with $\mathcal{O}(NL^3)$; however, we exploit an FFT to reduce this to $\mathcal{O}(NL^2 \log L)$.

Next, consider the Euler angle γ. We exploit the steerability of wavelet coefficients Eqn. (10), which transfers to $V_m(\beta,\gamma)$ directly, to compute integration over γ exactly and efficiently:

$$V_{mm'n} = \int_0^\pi \mathrm{d}\beta \sin\beta \, V_{mn}(\beta) \exp(-im'\beta) \,, \tag{38}$$

where

$$V_{mn}(\beta) = 2\pi z_n \sum_g V_m(\beta,\gamma_g) \exp(-in\gamma_g) \,, \tag{39}$$

which can be computed in $\mathcal{O}(N^2 L^2)$. The Euler angle γ is discretized according to the scheme specified in Sec. 3.1, where g denotes the index associated with γ.

Finally, consider the Euler angle β. Appealing to the quadrature rule Eqn. (17), which follows from the Driscoll and Healy sampling theorem, Eqn. (38) may be written:

$$V_{mm'n} = \sum_b q(\beta_b) V_{mn}(\beta_b) \exp(-im'\beta_b) \,, \tag{40}$$

which can be computed in $\mathcal{O}(NL^3)$. The Euler angle β is discretized according to the scheme specified in Sec. 3.1, where b denotes the index associated with β.

To summarise, the wavelet coefficient contribution to the function synthesis can be computed exactly by appealing to the quadrature rules outlined in Sec. 3.1. Furthermore, we have described a fast algorithm for this exact computation based on a factoring of rotations and separation of variables. This fast algorithm reduces the complexity of the computation from $\mathcal{O}(L^5)$ for the naive case to $\mathcal{O}(NL^3)$. Since $J+1$ wavelet scales are considered the overall complexity becomes $\mathcal{O}(JNL^3)$. However, again the compact support of the wavelets may be exploited so that the computation is dominated by the largest two scales, resulting in an overall complexity of effectively $\mathcal{O}(NL^3)$.

We finally consider the contribution to the function synthesis expression of Eqn. (4) from the scaling coefficients. Expressing this contribution in harmonic space one finds:

$$2\pi \int_{\mathbb{S}^2} \mathrm{d}\Omega(\omega')W^\Phi(\omega')(\mathcal{R}_{\omega'}L^\mathrm{d}\Phi)(\omega) = \sum_{\ell m} \sqrt{\frac{2\ell+1}{4\pi}} W^\Phi_{\ell m}\Phi_{\ell 0}Y_{\ell m}(\omega) \,. \tag{41}$$

The scaling coefficient contribution to the harmonic coefficients of the synthesized signal can thus be computed in $\mathcal{O}(L^2)$.

3.4 Numerical experiments

The exact and efficient algorithms described above to compute wavelet analysis and synthesis, *i.e.* forward and inverse wavelet transforms respectively, are implemented in the `S2DW`[§] package, which is publicly available. The `S2DW` package is written in `Fortran`, uses the `FFTW`[¶] to perform Fourier transforms, and (in version 1.1) is parallelized to run on multi-core architectures.[‖] Here we evaluate the accuracy and efficiency of `S2DW` up to extremely high band-limits ($L = 4096$), corresponding to functions sampled at tens of millions of pixels on the sphere. For reference, this band-limit exceeds the resolution of the recently released *Planck*[30] full-sky observations of the CMB.

We perform the following numerical experiments. For a given band-limit L, we generate random test signals f with harmonic coefficients uniformly randomly distributed in $[-1, 1]$. We compute all wavelet coefficients (up to the maximum possible wavelet scale $J = J_L(\alpha)$) by applying the wavelet analysis algorithm detailed in Sec. 3.2. We then synthesis the function from its wavelet coefficients by applying the wavelet synthesis algorithm detailed in Sec. 3.3. Numerical accuracy is evaluated by the maximum error between the original harmonic coefficients of f, denoted $f^{\mathrm{orig}}_{\ell m}$, and their synthesised values $f^{\mathrm{recon}}_{\ell m}$: $\epsilon = \max_{\ell,m} |f^{\mathrm{recon}}_{\ell m} - f^{\mathrm{orig}}_{\ell m}|$. Furthermore, we also record the wall-time clock τ for the combined analysis-synthesis computation. These numerical experiments are performed on a 2x Intel Xeon X5650 Processor (2.66Ghz, 12M Cache, 6.40 GT/s QPI, Turbo, HT) machine with 12 cores, where we perform 10 simulations for each band-limit considered.

The results of these numerical experiments are shown in Fig. 3. Firstly, notice that very good numerical accuracy is achieved (Fig. 3(a)), at the level of machine precision, up to very high band-limits. The numerical error is found empirically to scale as approximately $\mathcal{O}(L)$. Secondly, the algorithms discussed above are demonstrated to scale as $\mathcal{O}(L^3)$ (Fig. 3(b)) as predicted. Furthermore, the algorithms are sufficiently fast to allow computation up to very high band-limits in a reasonable time. These computation times are for version 1.1 of `S2DW` and are a considerable improvement over the computation time specified in Ref. 16 for version 1.0, due to parallelization, other code optimizations, and advances in computing hardware. For example, the round-trip computation time for $L = 1024$ is reduced from 72 minutes to less than 2 minutes.

[§] http://www.s2dw.org/

[¶] http://www.fftw.org/

[‖] The alternative `S2LET`[7] package (http://www.s2let.org/) provides a C implementation of scale-discretized wavelets, with Matlab interfaces. However, at present `S2LET` supports axisymmetric wavelets only.
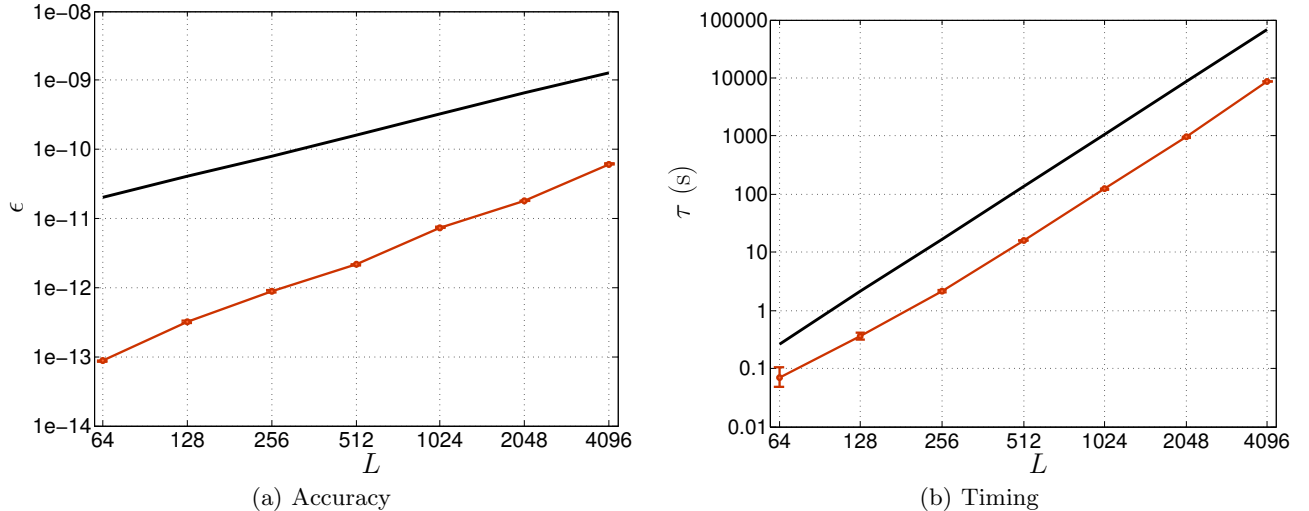
Figure 3. Computational performance of the `S2DW` implementation of the scale-discretized wavelet transform on the sphere ($N = 3$, $J = J_L(\alpha)$, $\alpha = 2$). In panel (a) the numerical error following a forward and inverse wavelet transform is shown. The algorithms described herein are theoretically exact and achieve close to machine precision for extremely large band-limits. Numerical error is found empirically to scale as approximately $\mathcal{O}(L)$, illustrated by the solid curve. In panel (b) the computation time of a forward and inverse wavelet transform is shown. As predicted, computation time is shown to scale as $\mathcal{O}(L^3)$, illustrated by the solid curve. In both panels the mean of 10 simulations is shown, with one standard deviation error bars. In most cases the errors bars are too small to be seen clearly.

4. SUMMARY AND FUTURE PERSPECTIVES

We have described exact and efficient algorithms to compute the wavelet analysis and synthesis of the scale-discretized wavelet transform on the sphere developed by Wiaux *et al.*.[16] These algorithms rely on the factoring of rotations approach[9, 28, 29] and a separation of variables. The compact support of the wavelets and azimuthal band-limit N may be exploited to further improve computational efficiency. Consequently, the cost of computing wavelet transforms is reduced from $\mathcal{O}(JL^5)$ for the naive setting to effectively $\mathcal{O}(NL^3)$, for both analysis and synthesis algorithms, *i.e.* for both the forward and inverse wavelet transforms.

The exactness of the algorithms is achieved by appealing to the Driscoll and Healy sampling theorem[24, 25] on the sphere. However, there is scope to further optimize this part of the algorithms, *i.e.* integrals and summations over θ and β. Recently, two of the authors of this article developed a novel sampling theorem on the sphere,[19] superseding the Driscoll and Healy sampling theorem. This new sampling theorem reduces the number of samples on the sphere required to represent a band-limited signal from $\sim 4L^2$ to $\sim 2L^2$. Furthermore, FFTs are exploited to yield fast algorithms to compute spherical harmonic transforms associated with the new sampling theorem rapidly.[19] In future work we plan to integrate these recent developments into the algorithms presented herein, replacing the use of the Driscoll and Healy sampling theorem with the new sampling theorem of Ref. 19. This will reduce the number of sample values required to represent wavelet coefficients (and functions on the sphere) by a factor of two, while retaining all of their information content, and will further improve the speed of the algorithms to compute the scale-discretized wavelet transform on the sphere.

ACKNOWLEDGMENTS

REFERENCES

[1] Planck Collaboration XXIII, "*Planck* 2013 results: Isotropy and statistics of the CMB," *Astron. & Astrophys.* (submitted, 2013).

[2] Simons, F. J., Loris, I., Nolet, G., Daubechies, I. C., Voronin, S., Judd, J. S., Vetter, P. A., Charléty, J., and Vonesch, C., "Solving or resolving global tomographic models with spherical wavelets, and the scale and sparsity of seismic heterogeneity," *Geophysical Journal International* **187**, 969–988 (Nov. 2011).

[3] Antoine, J.-P. and Vandergheynst, P., "Wavelets on the n-sphere and related manifolds," *J. Math. Phys.* **39**(8), 3987–4008 (1998).

[4] Antoine, J.-P. and Vandergheynst, P., "Wavelets on the 2-sphere: a group theoretical approach," *Applied Comput. Harm. Anal.* **7**, 1–30 (1999).

[5] Baldi, P., Kerkyacharian, G., Marinucci, D., and Picard, D., "Asymptotics for spherical needlets," *Annals of Statistics* **37 No.3**, 1150–1171 (2009).

[6] Marinucci, D., Pietrobon, D., Balbi, A., Baldi, P., Cabella, P., Kerkyacharian, G., Natoli, P., Picard, D., and Vittorio, N., "Spherical needlets for cosmic microwave background data analysis," *Mon. Not. Roy. Astron. Soc.* **383**, 539–545 (2008).

[7] Leistedt, B., McEwen, J. D., Vandergheynst, P., and Wiaux, Y., "S2LET: A code to perform fast wavelet analysis on the sphere," *Astron. & Astrophys.* (2012).

[8] McEwen, J. D., Hobson, M. P., and Lasenby, A. N., "A directional continuous wavelet transform on the sphere," *ArXiv* (2006).

[9] McEwen, J. D., Hobson, M. P., Mortlock, D. J., and Lasenby, A. N., "Fast directional continuous spherical wavelet transform algorithms," *IEEE Trans. Sig. Proc.* **55**(2), 520–529 (2007).

[10] Narcowich, F. J., Petrushev, P., and Ward, J. D., "Localized tight frames on spheres," *SIAM J. Math. Anal.* **38**(2), 574–594 (2006).

[11] Starck, J.-L., Moudden, Y., Abrial, P., and Nguyen, M., "Wavelets, ridgelets and curvelets on the sphere," *Astron. & Astrophys.* **446**, 1191–1204 (Feb. 2006).

[12] Wiaux, Y., Jacques, L., and Vandergheynst, P., "Correspondence principle between spherical and Euclidean wavelets," *Astrophys. J.* **632**, 15–28 (2005).

[13] Wiaux, Y., Jacques, L., Vielva, P., and Vandergheynst, P., "Fast directional correlation on the sphere with steerable filters," *Astrophys. J.* **652**, 820–832 (2006).

[14] Wiaux, Y., McEwen, J. D., and Vielva, P., "Complex data processing: fast wavelet analysis on the sphere," *J. Fourier Anal. and Appl.* **13**(4), 477–493 (invited contribution, 2007).

[15] Yeo, B., Ou, W., and Golland, P., "On the construction of invertible filter banks on the 2-sphere," *IEEE Trans. Sig. Proc.* **17**, 283–300 (march 2008).

[16] Wiaux, Y., McEwen, J. D., Vandergheynst, P., and Blanc, O., "Exact reconstruction with directional wavelets on the sphere," *Mon. Not. Roy. Astron. Soc.* **388**(2), 770–788 (2008).

[17] Hammond, D. K., Wiaux, Y., and Vandergheynst, P., "Wavelet domain Bayesian denoising of string signal in the cosmic microwave background," *Mon. Not. Roy. Astron. Soc.* **398**, 1317–1332 (Sept. 2009).

[18] Planck Collaboration XXV, "*Planck* 2013 results: Searches for cosmic strings and other topological defects," *Astron. & Astrophys.* (submitted, 2013).

[19] McEwen, J. D. and Wiaux, Y., "A novel sampling theorem on the sphere," *IEEE Trans. Sig. Proc.* **59**(12), 5876–5887 (2011).

[20] Varshalovich, D. A., Moskalev, A. N., and Khersonskii, V. K., [*Quantum theory of angular momentum*], World Scientific, Singapore (1989).

[21] Wiaux, Y., Jacques, L., and Vandergheynst, P., [*Wavelets on the sphere*], 131–174, Four Short Courses on Harmonic Analysis, Applied and Numerical Harmonic Analysis, Birkhauser, Boston (2010).

[22] McEwen, J. D., Wiaux, Y., Hobson, M. P., Vandergheynst, P., and Lasenby, A. N., "Probing dark energy with steerable wavelets through correlation of WMAP and NVSS local morphological measures," *Mon. Not. Roy. Astron. Soc.* **384**(4), 1289–1300 (2008).

[23] Vielva, P., Wiaux, Y., Martínez-González, E., and Vandergheynst, P., "Steerable wavelet analysis of CMB structures alignment," *New Astronomy Review* **50**, 880–888 (2006).

[24] Driscoll, J. R. and Healy, D. M. J., "Computing Fourier transforms and convolutions on the sphere," *Advances in Applied Mathematics* **15**, 202–250 (1994).

[25] Healy, D. M. J., Rockmore, D., Kostelec, P. J., and Moore, S. S. B., "FFTs for the 2-sphere – improvements and variations," *J. Fourier Anal. and Appl.* **9**(4), 341–385 (2003).

[26] McEwen, J. D., Puy, G., Thiran, J.-P., Vandergheynst, P., Ville, D. V. D., and Wiaux, Y., "Sampling theorems and compressive sensing on the sphere," in [*Wavelets and Sparsity XIV, SPIE international symposium on optics and photonics*], (2011).

[27] Górski, K. M., Hivon, E., Banday, A. J., Wandelt, B. D., Hansen, F. K., Reinecke, M., and Bartelmann, M., "Healpix – a framework for high resolution discretization and fast analysis of data distributed on the sphere," *Astrophys. J.* **622**, 759–771 (2005).

[28] Risbo, T., "Fourier transform summation of Legendre series and D-functions," *J. Geodesy* **70**(7), 383–396 (1996).

[29] Wandelt, B. D. and Górski, K. M., "Fast convolution on the sphere," *Phys. Rev. D.* **63**(12), 123002 (2001).

[30] Planck Collaboration I, "*Planck* 2013 results: Overview of Planck Products and Scientific Results," *Astron. & Astrophys.* (submitted, 2013).